# Pressure dependence of metal-insulator transition in perovskites $R$NiO$_3$ ($R$=Eu, Y, Lu)

J.-G. Cheng,[1] J.-S. Zhou,[1,*] J. B. Goodenough,[1] J. A. Alonso,[2] and M. J. Martinez-Lope[2]
[1]*Texas Materials Institute, University of Texas at Austin, Austin, Texas 78712, USA*
[2]*Instituto de Ciencia de Materiales de Madrid (CSIC), Cantoblanco, 28049 Madrid, Spain*
(Received 1 June 2010; published 11 August 2010)

High-pressure experiments on the $R$NiO$_3$ perovskites with smaller rare-earth $R^{3+}$ ions complete our study of the crossover from itinerant to localized $e$-electron behavior associated with the low-spin Ni(III):$t^6e^1$ ion. By measuring second-sintered samples in a multianvil module, we have observed a clear anomaly of $\rho(T)$ at $T_{\mathrm{IM}}$ and obtained the pressure dependence of $T_{\mathrm{IM}}$ for the $R$NiO$_3$ ($R$=Eu, Y, Lu) that are different from the published data supporting a charge-ordering model. Instead, they are comparable to that for the orbital-ordering insulator LaMnO$_3$. Our distinct results show clearly that where the crossover is approached from the localized-electron side by increasing the orbital overlap integral, a cooperative Jahn-Teller distortion prevents charge transfer from molecular $e$ orbitals on strongly bonded NiO$_{6/2}$ clusters to more weakly bonded Ni(III) centers. However, where the crossover is approached from the itinerant-electron side as in the perovskite CaFeO$_3$, a disproportionation charge transfer may occur. In a separate experiment in which the powder samples were pressed in a Bridgman anvil device without a pressure medium, we have shown after releasing pressure that the samples were reduced. This irreversible effect should be distinguished from the hydrostatic-pressure effect on the physical properties of the $R$NiO$_3$ perovskites.

DOI: 10.1103/PhysRevB.82.085107 PACS number(s): 71.27.+a, 71.28.+d, 71.30.+h, 72.80.Ga

## I. INTRODUCTION

The perovskite family $R$NiO$_3$ provides an opportunity to study the transition from itinerant to localized 3$d$-electron behavior[1] in a system with (180°−$\phi$) Ni-O-Ni interactions where a single electron per Ni(III) in a low-spin state $t^6e^1$ occupies, in cubic site symmetry, a twofold-degenerate orbital in which the orbital angular momentum is quenched. Moreover, it is instructive to contrast the behavior of the $e$ electrons in the $R$NiO$_3$ family with those in the perovskites CaFeO$_3$ and LaMnO$_3$ since high-spin octahedral-site Fe(IV) and Mn(III) each also have a single $e$ electron in a $t^3e^1$ manifold but in the presence of a localized spin $S$=3/2 from the $t^3$ electrons.

The end member LaNiO$_3$ of the $R$NiO$_3$ family is rhombohedral $R\bar{3}c$; this structure does not lift the $e$-orbital degeneracy, and LaNiO$_3$ remains metallic with an enhanced Pauli paramagnetism to lowest temperature.[2] In this compound, the covalent component of the Ni-O bonding is strong enough that the interactions of the $\sigma$-bonding ligand-field $e$ orbitals across the bridging oxygen make the $e$ electrons occupy a narrow $\sigma^*$ band of itinerant electron states. However, as shown in Fig. 1(a), the orthorhombic $Pbnm$ members of the $R$NiO$_3$ family[3] exhibit an insulator-conductor transition at a $T_{IM}$ that increases with decreasing ionic radius (IR) of the $R^{3+}$ ion from Pr to Gd. The insulator phase becomes antiferromagnetic below a Néel temperature $T_{\mathrm{N}}$ that increases with increasing IR until it intersects $T_{\mathrm{IM}}$ in the Sm$_{1-x}$Nd$_x$NiO$_3$ system. A first-order expansion of the lattice occurs on either traversing the $R\bar{3}c$ to $Pbnm$ transition or crossing the metallic to insulator phase within the $Pbnm$ structure[3]; but on cooling through the $T_{\mathrm{IM}}>T_{\mathrm{N}}$ transition temperature, no anomaly could be detected in the Curie-Weiss paramagnetism of the Sm$_{0.5}$Nd$_{0.5}$NiO$_3$ sample.[2] Under hydrostatic pressure, the $T_{\mathrm{IM}}=T_{\mathrm{N}}$ of PrNiO$_3$ decreases dramatically and vanishes through a first-order transition to a quantum-critical-point phase.[4]

The insulator phase below $T_{\mathrm{IM}}$ is monoclinic $P2_1/n$ with two distinguishable Ni sites, one with a shorter and the other with a longer mean Ni-O bond length.[5,6] This observation led to the assumption that a charge disproportionation 2Ni(III)=Ni$^{3-\delta}$+Ni$^{3+\delta}$, i.e., a negative-$U$ charge-density wave, sets in below $T_{\mathrm{IM}}$. Such a disproportionation reaction would be analogous to the reaction 2Fe(IV) =Fe(III)+Fe(V) occurring in CaFeO$_3$ below a $T_{\mathrm{IM}}\approx 240$ K that has been conclusively demonstrated by a neutron-diffraction study.[7] However, structural studies of the $R$NiO$_3$ with smaller IR have shown a large Jahn-Teller (JT) distortion of the larger Ni site below $T_{\mathrm{IM}}$ characteristic of a localized $e$ electron on Ni(III):$t^6e^1$; no such distortion would be expected at a Ni(II):$t^6e^2$ or a Ni(IV):$t^6e^0$ site. Thus, it appears that the $e$ electrons of the Ni(III) in the $R$NiO$_3$ with smaller IR remain localized to a site but there is a displacement of the oxygen that distinguishes the covalent bonding with the $e$ orbitals on the two Ni(III)O$_{6/2}$ sites.[8]

In contrast to orthorhombic CaFeO$_3$, which is metallic above its $T_{\mathrm{IM}}$,[9] orthorhombic LaMnO$_3$ is a polaronic conductor[10] in its high-temperature phase and undergoes a cooperative Jahn-Teller distortion of the Mn(III) sites below a $T_{\mathrm{JT}}>T_{\mathrm{N}}$.[11] Figure 1(b) shows the phase diagram for the $R$MnO$_3$ family to illustrate that the transition temperatures in the two opposite end members, LuNiO$_3$ and LaMnO$_3$, are similar. From the transitions in CaFeO$_3$ and LaMnO$_3$, we see that the disproportionation reaction removes the orbital degeneracy of a narrow $\sigma^*$ band of $e$-orbital parentage whereas a cooperative Jahn-Teller distortion removes the $e$-orbital degeneracy of localized electrons.

In a recent report, Mazin *et al.*[12] have put forward a model, based on high-pressure transport data for LuNiO$_3$, that a disproportionation, or charge ordering (CO), is more favorable than the cooperative Jahn-Teller distortion, or orbital ordering (OO), in "an intermediate phase between a strongly localized and an itinerant regime." Their data, however, do not show whether $\rho(T)$ has an anomaly at $T_{\mathrm{IM}}$ and

 

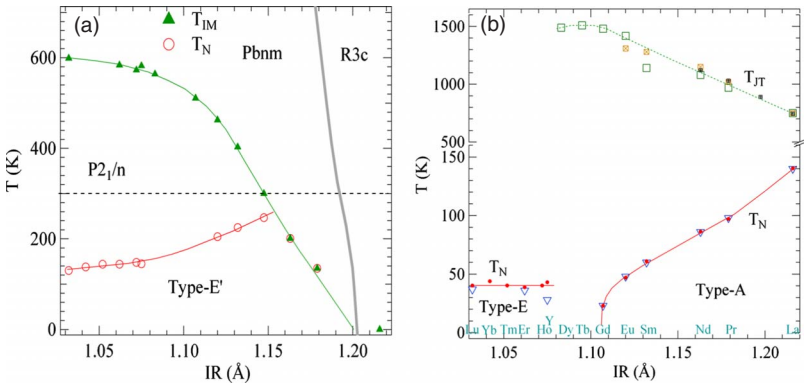


FIG. 1. (Color online) Phase diagram of two perovskite families (a) $R\mathrm{NiO_3}$ and (b) $R\mathrm{MnO_3}$. Lines through data points are guides to the eyes. The phase boundary between the *Pbnm* phase and the $R\bar{3}c$ phase in (a) is based on the data in Ref. 34.

how $T_{IM}$ is suppressed under pressure; these data are critical to distinguish the CO insulator from the OO insulator below $T_{IM}$. Suppressing the first-order insulator-to-metal transition requires a rather high pressure; 32 GPa in the OO insulator $LaMnO_3$.[13] In contrast, the CO phase is better described as a band insulator below $T_{IM}$, and one should then observe under pressure "a semiconducting behavior with the gap smoothly going to zero and disappearing at the transition."[12] However, testing these two models on the perovskite nickelates turns out to be not so easy because of some chemical issues.

The synthesis of chemically stoichiometric $R\mathrm{NiO_3}$ requires high oxygen pressure. A 200 bar oxygen pressure achieved in a high-pressure gas furnace is sufficient to synthesize the $R\mathrm{NiO_3}$ members for $R$=La to Eu. Hard-pellet samples obtained directly from the high-oxygen-pressure synthesis can be used to measure transport properties. However, for compounds with a smaller IR, a high-pressure synthesis above 2 GPa with a solid-state pressure medium must be used.[14,15] In this case, the starting materials are mixed with an oxygen-releasing agent, e.g., $KClO_4$, and sealed in a Au or Pt crucible before being loaded into a press. A high-purity perovskite phase can be obtained by grinding the high-pressure product and washing with diluted acid and water. However, it is difficult to make dense pellets for the measurement of transport properties since sintering at high temperatures is accompanied by loss of oxygen. Therefore, differential scanning calorimetry (DSC) has been used to monitor the $T_{IM}$ transition temperature in these as-made powder samples. Since the temperature of the DSC anomaly matches well that of the sharp transition of $\rho(T)$ at $T_{IM}$ for $SmNiO_3$,[14,16] the anomaly from the DSC has been used to track $T_{IM}$ versus IR over the whole phase diagram shown in Fig. 1(a). Three questions remain open for the nickelates with a smaller IR: (1) does $\rho(T)$ change abruptly at $T_{IM}$? (2) How does $\rho(T)$ below $T_{IM}$ change with pressure? (3) How does $T_{IM}$ change with pressure? One more factor needed to be considered in designing experiments at high temperatures is oxygen stoichiometry in the sample, which may change during the measurement.

Mazin *et al.*[12] measured the temperature dependence of the resistance on a powder sample $LuNiO_3$ in a diamond-anvil cell (DAC) below room temperature. They have shown in Fig. 3(a) of their paper a peculiar behavior of $R(T)$ versus pressure below 300 K. At 2.7 GPa, for example, $R(T)$ undergoes a broad maximum at a $T_{max}$ that increases with pressure until it saturates at $P>5$ GPa. With the same technique, an apparent gradual closing of an energy gap was also reported for $EuNiO_3$ under pressure.[17] However, no such behavior has been seen in the $\rho(T)$ versus pressure data for $R\mathrm{NiO_3}$ ($R=Sm_{0.5}Nd_{0.5}$ with $T_{IM}>T_N$ and $R$=Nd, Pr with $T_{IM}=T_N$) where a well-defined $T_{IM}$ decreases monotonically with pressure.[18] Since $T_{IM}$ at atmospheric pressure changes smoothly as a function of IR between $EuNiO_3$ and $SmNiO_3$, we were motivated to check whether a gradual closing of an energy gap does, in fact, occur under an applied pressure.

## II. EXPERIMENT

Powder samples of $R\mathrm{NiO_3}$ ($R$=Eu, Y, Lu) were prepared under high pressure and high temperature. The detailed procedure can be found in previous publications.[14,15] In order to obtain highly dense pellets, the powder samples were sintered again at 4 GPa oxygen pressure and 900 °C for 20 min. In this sinter, the sample pellets and $KClO_4$ sealed in a Au crucible were separated by a thin layer of Y-stabilized $ZrO_2$ so that oxygen can penetrate through the $ZrO_2$ barrier while KCl remains separated from the sample. X-ray powder diffraction shows that the samples after the second sintering have the same lattice parameters as that from the first sintering. Thermoelectric power, $S$, is extremely sensitive to the chemical stoichiometry for insulator samples and is not influenced by the contact issue at grain boundaries. All the as-made samples and the second-sintering samples show $S\approx-300$ $\mu$V/K at room temperature, which is consistent with an insulator ground state for these nickelates. We have carried out both the second sintering and $R(T)$ measurements under high pressure and high temperature (HPHT) in a Walker-type multianvil module (Rockland Research) that is placed in a 500-Ton hydraulic press. The assembly for $R(T)$ measurements is shown in Fig. 2; it has a quasifour-probe configuration. This configuration can get rid of any contribution from the leads but it still includes the contact resistance between the sample and leads. However, the contact resistance is on the order of a couple of ohms and is reduced significantly under pressure. It is negligible in comparison with the $R(T)$ from high-resistance samples such as the $R\mathrm{NiO_3}$ perovskites in this study. The $T_{IM}$ for the $R\mathrm{NiO_3}$ samples and the $T_{JT}$ from $LaMnO_3$ obtained with this method are consistent with those obtained with DSC or a standard four-probe resistance measurement at ambient pressure. Since the sample is not protected with a Au crucible in the $R(T)$ measurement under HPHT, chemical stoichometry may

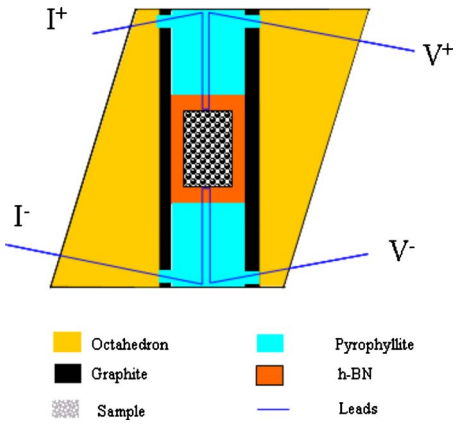


FIG. 2. (Color online) Schematic drawing of the configuration for a resistivity measurement under high temperature and high pressure in a multianvil module.

have been changed during the measurement. We have checked the samples recovered after the measurement by x-ray diffraction (XRD) and by a thermoelectric-power measurement. The lattice parameters from XRD in Fig. 3 show no noticeable change and the absolute value of $S$ shown below is only slightly reduced. We have found that the hexagonal BN sleeve plays a critical role to keep the sample's oxygen stoichiometry. This soft material is used to provide quasihydrostatic pressure around the sample. Therefore, the sample recovered after the measurement up to 10 GPa has exactly the same shape it had when it was loaded. As we discuss below, nonhydrostatic pressure creates some shear stress that causes a serious problem for the chemistry of the nickelates. The resistivity measurements at ambient pressure were made with a standard four-probe method and the thermoelectric power measurements were performed in a homemade apparatus.

## III. RESULTS AND DISCUSSION

The temperature dependences of resistivity of the $R\mathrm{NiO_3}$ ($R$=Eu, Y, Lu) samples shown in Fig. 4 reveal important information about the transition at $T_{\mathrm{IM}}$ for the $R\mathrm{NiO_3}$ family with smaller IR. The major features are these: (1) the resistivity indeed undergoes a dramatic change at $T_{\mathrm{IM}}$ where the DSC shows an anomaly; (2) the transition at $T_{\mathrm{IM}}$ is not particularly sensitive to high pressure; $T_{\mathrm{IM}}$ stays well above 500 K under 10 GPa for $\mathrm{LuNiO_3}$; (3) $\rho(T)$ at $T>T_{\mathrm{IM}}$ does not behave as a typical metal but it approaches metallic behavior under higher pressures; (4) $\rho(T)$ increases dramatically below $T_{\mathrm{IM}}$. In contrast, the transition at $T_{\mathrm{IM}}$ reported by Mazin *et al.*[12] cannot be defined from their measurements of $R(T)$ under different pressures. According to their phase diagram, the metallic phase should extend to room temperature at 10 GPa for $\mathrm{LuNiO_3}$. Before discussing the implications of our data, we have to clarify a critical issue, viz., why samples coming from the same source (CSIC) show different behavior in the different high-pressure measurements.

The second sintering made at UT Austin was performed to make a well-sintered and dense pellet but it does not alter the

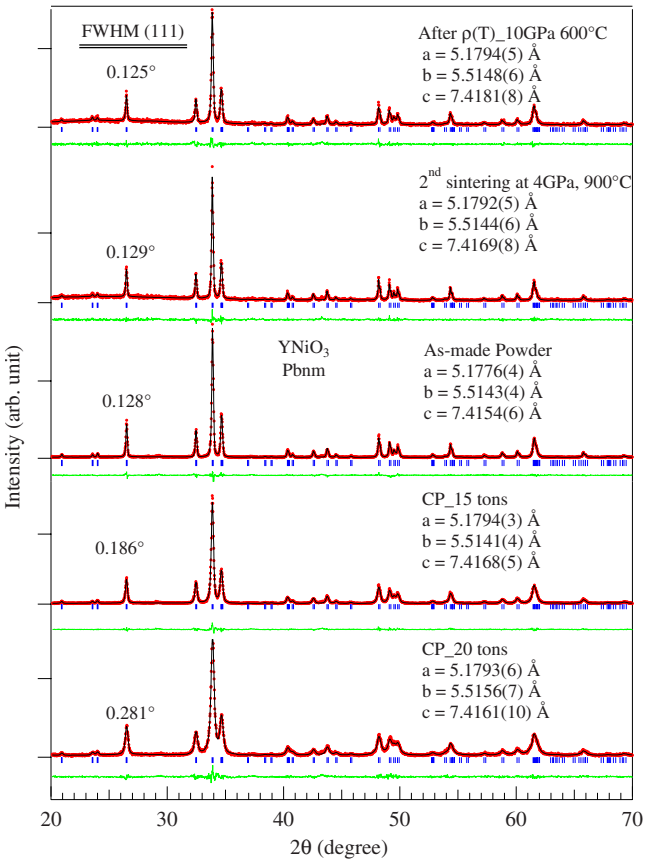


FIG. 3. (Color online) X-ray powder diffraction data for samples made by different procedures. CP stands for cold pressing. Numbers on the left-hand side inside the plot are the FWHM for the (111) diffraction. All data are given together with the results of a Rietveld refinement by using the *Pbnm* space group. The monoclinic distortion is extremely small at room temperature. Refinements of the XRD data with $P2/n$ and *Pbnm* do not result in any difference.

crystal structure and chemistry as mentioned in the experimental part. Moreover, a sample recovered from the $\rho(T)$ under HPHT does not show any change in the crystal structure and has only a slightly reduced thermoelectric power, which signals that the high-temperature behavior of $\rho(T)$ shown in Fig. 4 is the intrinsic property of $R\mathrm{NiO_3}$. In the report by Mazin *et al.*,[12] what happens to the sample after releasing pressure has not been mentioned. A diamond-anvil cell was used in their work for measuring the resistivity under pressure. No pressure medium has been specified in the report. We have performed the following experiments to test what happens to the nickelate under a strong uniaxial pressure. As shown in the inset of Fig. 5, the powder samples were placed in a hole drilled in a hard cardboard as a gasket that was loaded between two tungsten carbide (WC) anvils of 1.2 cm diameter. The loading force to 20 tons generates about 0.5 GPa, an average pressure between anvils; but the pressure at the central location can reach to about 2 GPa. The pellets recovered from the pressing had good mechanical strength. The XRD peaks of the hard pellets shown in Fig. 3 are broadened a little relative to that of the powder samples before pressing. However, the thermoelectric power from the pellets, $\mathrm{YNiO_3}$ in Fig. 5(a) for example, is significantly lower

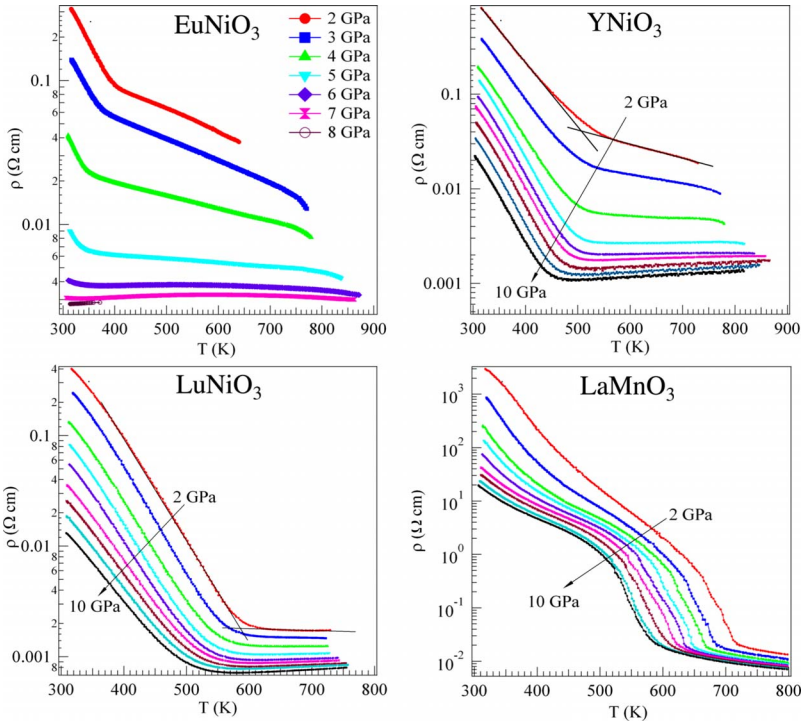


FIG. 4. (Color online) Temperature dependence of resistivity for $R\mathrm{NiO_3}$ ($R$=Eu, Y, Lu) and $\mathrm{LaMnO_3}$. Transition temperatures at $T_{\mathrm{IM}}$ and $T_{\mathrm{JT}}$ inside the figure are defined as illustrated in $\mathrm{LuNiO_3}$ at 2 GPa.

than that of the original powder samples. We have done the same experiment on all other samples of $R\mathrm{NiO_3}$ from $R$ =Pr to Lu. $\mathrm{NdNiO_3}$ of Fig. 5(a) is a typical example for the $R\mathrm{NiO_3}$ with larger IR. These samples all have a relatively small absolute value of $S$ regardless of a metallic phase or an insulator phase, and they exhibit no anomaly in $S(T)$ at $T_{\mathrm{IM}}$. The cold-pressed sample of $\mathrm{YNiO_3}$ in Fig. 5(b) also shows a less dramatic temperature-dependent resistance below $T_{\mathrm{IM}}$ than the sample after the second sintering. As checked by the magnetic susceptibility, $T_{\mathrm{N}}$ from these cold-pressed samples, however, shows more or less no change relative to that from the as-made samples. A significantly reduced absolute value of $S$ from the cold-pressed samples indicates that the sample is doped with more charge carriers after the cold pressing. Thermogravimetric analysis was used to verify this conjecture. As shown in Fig. 6, the overall weight loss during decomposition to $R_2\mathrm{O_3}$ and nickel metal is nearly the same for both an as-made sample and a cold-pressed sample. But the detail of how the weight changes as a function of temperature differs quite a lot between the two samples. The decomposition temperature of the cold-pressed sample is lower by over 100 °C, which is indicative of a much smaller grain size in the sample. The sample begins to lose oxygen upon heating from room temperature. The oxygen loss at such a low temperature must be from the grain boundaries, which is why the cold-pressed sample is slightly electron doped. This result is highly consistent with the change in $S$ from −300 to −50 $\mu\mathrm{V/K}$ between these two samples. The chemical stoichiometry in these cold-pressed samples can be restored by performing the second sintering under high oxygen pressure. High-quality transport data showing low resistivity in the conductive phase and an extremely sharp transition at $T_{\mathrm{IM}}$ from both $\rho(T)$ and $S(T)$ have been obtained, respectively, on these cold-pressed and reannealed samples.[2,4,17] It has also been found that high-pressure measurements made in a large-volume, liquid-filled chamber in a piston-cylinder device do not alter the doped state in the nickelates. In the case of the DAC, the final gap between anvils is very tiny for $P>10$ GPa. In this case, the sample may make contact with the two anvils and become subject to some uniaxial pressure even where the chamber is filled with some pressure medium. A good example to show this uniaxial pressure effect in a DAC is from a comparison between two high-pressure experiments on $\mathrm{BaFe_2As_2}$;[19] one was done with a modified Bridgman device and the other with a cubic multianvil module. The onset of superconductivity in $\mathrm{BaFe_2As_2}$ is extremely sensitive to uniaxial pressure along the $c$ axis. A $c$-axis-oriented flake of the crystal placed in the Bridgman device shows superconductivity at a much lower pressure $P_{\mathrm{c}}$ than that used in a multianvil module. Our experience in handling nickelates samples is that the sample's chemistry is not altered only if the sample recovered from a high-pressure experiment has exactly the same shape as it had before loading into the pressure chamber.

The influence on $\rho(T)$ and $T_{\mathrm{N}}$ by doping charge carriers into $R\mathrm{NiO_3}$ perovskites has been studied independently by two groups; one group[20,21] used chemical substitutions and the other group[22] changed the oxygen stoichiometry. Whereas $T_{\mathrm{IM}}$ shows almost no change, the resistivity below $T_{\mathrm{IM}}$ in the $\mathrm{NdNiO_{3-\delta}}$ sample was reduced dramatically as $\delta$ increased,[22] which is precisely what we have observed in the cold-pressed samples. We have concluded that pressing at room temperature under uniaxial pressure creates fine-size grains in which part of the lattice oxygen are converted into peroxide surface species at the grain boundaries to make the sample slightly electron doped at room temperature. By measuring these slightly reduced samples at ambient pressure, we can reproduce the essential features in results reported by Mazin *et al.*[12]

After clarifying that the true pressure effect on the physical properties of the nickelates can only be obtained if the

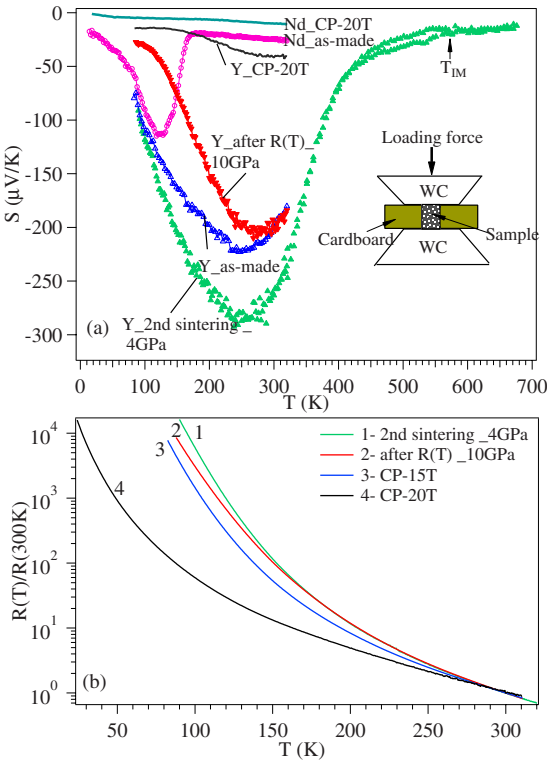


FIG. 5. (Color online) (a) Temperature dependence of thermoelectric power for $R\mathrm{NiO_3}$ ($R$=Nd, Y). Cold-pressing (CP) treatment has been used on all $R\mathrm{NiO_3}$ samples. The second sintering and $\rho(T)$ measurement under pressure have been made only on the $R\mathrm{NiO_3}$ with $R$=Eu, Y, and Lu. The $S(T)$ of $\mathrm{YNiO_3}$ is selected to show typical changes after different treatments. $T_{\mathrm{IM}}$ shown in the figure is from DSC measurement. $S(T)$ of $\mathrm{YNiO_3}$ shows an anomaly similar to that of $\mathrm{NdNiO_3}$ at $T_{\mathrm{IM}}$. The cold-pressing changes these samples dramatically: (1) the anomaly of $S(T)$ at $T_{\mathrm{IM}}$ disappears in the CP $\mathrm{NdNiO_3}$; (2) the absolute value of $S(T)$ of the CP $\mathrm{YNiO_3}$ is significantly reduced. The inset shows a schematic drawing of the cold-pressing device. (b) Temperature dependence of the resistance normalized by the value at room temperature for $\mathrm{YNiO_3}$ after different treatments.

nickelate samples are measured under hydrostatic or quasi hydrostatic pressure, we are in a position to discuss implications of our high-pressure results. For all perovskites $R\mathrm{NiO_3}$ from $R$=La to Lu, the resistivity of the phase at $T>T_{\mathrm{IM}}$ is relatively small with a weak temperature dependence. The conductive phase above $T_{\mathrm{IM}}$ shows an evolution from a well-defined metal [Fermi-liquid behavior has been found at low temperatures in $\mathrm{LaNiO_3}$ (Ref. 4)] for larger IR to a semiconductor phase for smaller IR. The transition at $T_{\mathrm{IM}}$ in $\mathrm{LuNiO_3}$ is an insulator-semiconductor transition like the transition at $T_{\mathrm{JT}}$ in $\mathrm{LaMnO_3}$. Moreover, the transition at $T_{\mathrm{IM}}$ progressively loses its sharpness and thermal hysteresis as the IR decreases with $T_{\mathrm{IM}}>T_{\mathrm{N}}$. Also, as $T_{\mathrm{IM}}>T_{\mathrm{N}}$ increases, the paramagnetic susceptibility of the high-temperature phase exhibits a continuous evolution from the enhanced Pauli paramagnetism of $\mathrm{LaNiO_3}$ to a Curie-Weiss $\chi(T)$ for $\mathrm{LuNiO_3}$.[2,23,24] In Fig. 7, we have summarized the pressure dependence of $T_{\mathrm{IM}}$ and compared it to that of $T_{\mathrm{JT}}$ for $\mathrm{LaMnO_3}$. The data showing the evolution of $dT_{\mathrm{IM}}/dP$ as a function of IR also divides the

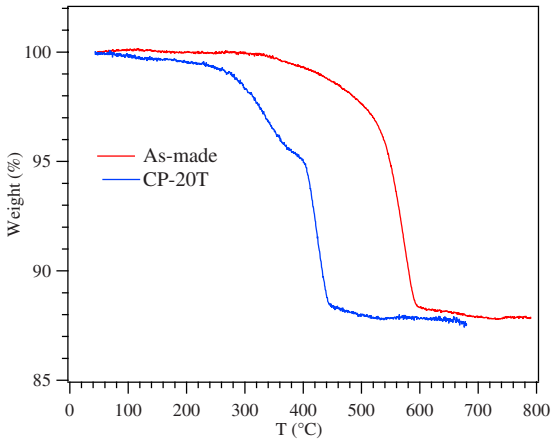


FIG. 6. (Color online) The weight change as a function of temperature of two $\mathrm{YNiO_3}$ samples. The measurements were performed in a mixture of 5% $\mathrm{H_2}$/95%Ar gas.

phase diagram into two distinct groups; compositions with smaller IR and $T_{\mathrm{IM}}>T_{\mathrm{N}}$ show a $T_{\mathrm{IM}}$ less sensitive to pressure such as the $T_{\mathrm{JT}}$ of $\mathrm{LaMnO_3}$ whereas those with $T_{\mathrm{IM}}=T_{\mathrm{N}}$ have a $T_{\mathrm{IM}}$ that decreases much more steeply with pressure.[18,25,26]

The transition from itinerant-electron states in a narrow $\sigma^*$ band of width $W_\sigma$ to localized $e$ electrons occurs where the on-site correlation energy $U$ is $U\approx W_\sigma$. The thermally driven $d$-electron transition in an oxide is normally first order if it occurs at low temperatures. An ordered phase segregation may be manifest in a single-valent system as a clustering into cation clusters or, in the case of transition-metal $M$ at-

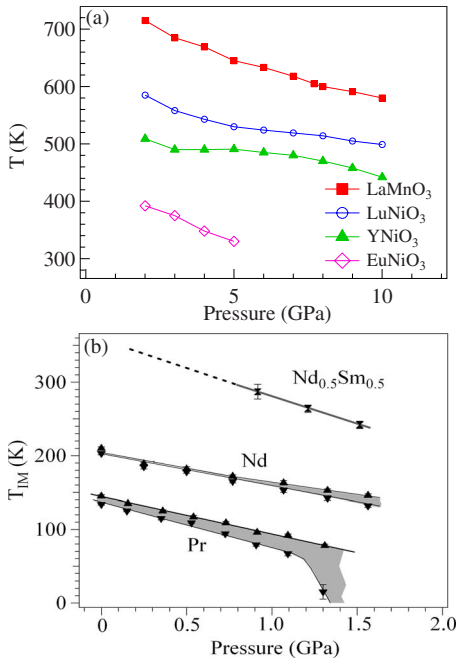


FIG. 7. (Color online) (a) Pressure dependence of the conductor-insulator transition temperature $T_{\mathrm{IM}}$ for $R\mathrm{NiO_3}$ ($R$=Eu, Y, Lu) and $T_{\mathrm{JT}}$ for $\mathrm{LaMnO_3}$, (b) pressure dependence of the metal-insulator transition for $R\mathrm{NiO_3}$ ($R$=Pr, Nd, $\mathrm{Nd_{0.5}Sm_{0.5}}$). The shadow areas represent the hysteresis loop between the measurements on cooling down and warming up.

oms in a perovskite structure, into alternating larger and smaller $MO_{6/2}$ sites as a result of cation-anion clustering. There are two possibilities to characterize cation-anion clusters. As the crossover is approached from the itinerant electron side, the on-site Coulomb energy $U$ is relatively small and is overcompensated by a gain of the bonding energy for a charge-disproportionation reaction such as 2Fe(IV) $=$Fe(III)$+$Fe(V) in $CaFeO_3$. In this case, the transition of $\rho(T)$ at $T_t$ appears to be second order.[9] But the most conclusive evidence is from the structural data;[7] $FeO_{6/2}$ at both Fe sites show a negligible bond-length splitting that is highly consistent with non-JT active ions of Fe(III):$t^3e^2$ and Fe(V):$t^3e^0$. The same structure has been reported in another charge disproportionation perovskite $BaBiO_3$.[27] In contrast, the phase segregation into the formation of $MO_{6/2}$ sites containing molecular $e$ orbitals separated by M atoms containing localized $e$ electrons occurs as the crossover is approached from the localized electron side.[28] In this case, Jahn-Teller distortions associated with the localized $e$ orbitals and the energy $U$ raise the empty $e$ orbitals on the localized-electron sites above the occupied $e$ orbitals on the molecular-orbital sites, which prevents the charge disproportionation. A significantly larger bond-length splitting[5] than that due to the intrinsic site distortion found on the larger of two Ni sites in the highly distorted $RNiO_3$ is a key factor to attribute $T_{IM}$ to the JT transition. As a matter of fact, structural data reported by Mazin *et al.*[12] also show clearly the JT distortions at Ni;[1] the distortions remain to the highest pressure 8 GPa in that study. In addition, the feature of $\rho(T)$ at $T_{IM}$ and the pressure dependence $dT_{IM}/dP$ are similar to the transition at $T_{JT}$ in $LaMnO_3$. Although $LaMnO_3$ approaches crossover,[29] it is not close enough to crossover at atmospheric pressure to induce a segregation into formation of $MnO_{6/2}$ strongly bonded clusters separated by a localized-electron Mn(III) ion. In the $RNiO_3$ family, there may be a crossover from a CO charge transfer below $T_{IM}$ in Pr and Nd where crossover is approached from the itinerant-electron side but in the $RNiO_3$ perovskites with an IR smaller than that of $R$=Eu, as is the case for $LuNiO_3$, the crossover is approached from the localized-electron side. Moreover, a $dT_N/dP>0$ found for these nickelates with $T_N$ increasing as IR increases is fundamentally against a band-electron model.[1] A $d \ln T_N/dP = 3.3\times10^{-2}$ GPa obtained for $LuNiO_3$ (Ref. 11) and a similar value for other $RNiO_3$ (Ref. 30) with $T_{IM}>T_N$, however, can be well-justified quantitatively by the Bloch rule[31] for an antiferromagnetic insulator with the superexchange interaction given the compressibility of nickelate obtained for $SmNiO_3$ (Ref. 32) and $YNiO_3$.[33]

## IV. CONCLUSION

The orthorhombic $RNiO_3$ perovskites containing low-spin Ni(III):$t^6e^1$ ions are metastable at ambient pressure and provide an opportunity to study the transition from itinerant to localized $e$ electrons with IR of the rare-earth $R^{3+}$ ions. Comparison of the properties of the orthorhombic $RNiO_3$ compounds with those of $LaMnO_3$ and $CaFeO_3$ is instructive since the $e$ electrons of the Mn(III) are localized and undergo a cooperative Jahn-Teller distortion of the $MnO_{6/2}$ sites at an insulator-conductor transition at a $T_{JT}$ and $CaFeO_3$ undergoes a CO disproportionation reaction of the Fe(IV) below an insulator-metal transition at a $T_{IM}$. $LaMnO_3$ approaches the crossover to itinerant $e$-electron behavior and $CaFeO_3$ approaches the crossover to localized $e$-electron behavior. As for the nickelates, none of the features predicted for a CO phase have been observed in our high-pressure experiments. Instead, we have observed a well-defined $T_{IM}$ from the resistivity measurements for the entire family. The pressure dependence of $T_{IM}$, however, divides the family into two groups. For those $RNiO_3$ with smaller IR, the behaviors of $\rho(T)$ at $T_{IM}$ and $dT_{IM}/dP$ are similar to those found in $LaMnO_3$, which indicates clearly that localized $e$ electrons undergo a cooperative Jahn-Teller distortion but stronger Ni-O bonding in alternate $NiO_{6/2}$ octahedra creates molecular $e$ orbitals within the more strongly bonded clusters as a result of the approach to crossover to itinerant-electron behavior from the localized-electron side.

Our data and conclusions differ from those recently reported for $LuNiO_3$. We have shown that the bulk oxygen stoichiometry does not change in our high-pressure experiments, which were done under quasihydrostatic pressure. In contrast, in the absence of a pressure medium, oxygen are displaced from the bulk to the grain surfaces so as to dope charge carriers to the bulk under strong uniaxial pressure, which may contribute to the pressure-induced change in resistance recently reported for $LuNiO_3$.

## ACKNOWLEDGMENT

This work was supported by NSF (Grant No. DMR 0904282) and the Robert A Welch foundation (Grant No. F-1066) in the USA and by Spanish Ministry of Science and Innovation (Grant no. MAT 2007-60536) in Spain.

*jszhou@mail.utexas.edu

[1] J. B. Goodenough, Phys. Rev. **164**, 785 (1967).
[2] J.-S. Zhou, J. B. Goodenough, B. Dabrowski, P. W. Klamut, and Z. Bukowski, Phys. Rev. Lett. **84**, 526 (2000).
[3] J. B. Torrance, P. Lacorre, A. I. Nazzal, E. J. Ansaldo, and Ch. Niedermayer, Phys. Rev. B **45**, 8209 (1992).
[4] J.-S. Zhou, J. B. Goodenough, and B. Dabrowski, Phys. Rev. Lett. **94**, 226602 (2005).
[5] J. A. Alonso, J. L. Garcia-Munoz, M. T. Fernandez-Diaz, M. A. G. Aranda, M. J. Martinez-Lope, and M. T. Casais, Phys. Rev. Lett. **82**, 3871 (1999).
[6] M. Medarde, M. T. Fernandez-Diaz, and Ph. Lacorre, Phys. Rev. B **78**, 212101 (2008).
[7] P. M. Woodward, D. E. Cox, E. Moshopoulou, A. W. Sleight, and S. Morimoto, Phys. Rev. B **62**, 844 (2000).
[8] J.-S. Zhou and J. B. Goodenough, Phys. Rev. B **69**, 153105

(2004).
[9] M. Azuma, T. Saito, S. Ishiwata, I. Yamada, Y. Kohsaka, H. Takagi, and M. Takano, Physica C **392-396**, 22 (2003).
[10] J.-S. Zhou and J. B. Goodenough, Phys. Rev. B **60**, R15002 (1999).
[11] J. Rodríguez-Carvajal, M. Hennion, F. Moussa, A. H. Moudden, L. Pinsard, and A. Revcolecschi, Phys. Rev. B **57**, R3189 (1998).
[12] I. I. Mazin, D. I. Khomskii, R. Lengsdorf, J. A. Alonso, W. G. Marshall, R. M. Ibberson, A. Podlesnyak, M. J. Martinez-Lope, and M. M. Abd-Elmeguid, Phys. Rev. Lett. **98**, 176406 (2007).
[13] I. Loa, P. Adler, A. Grzechnik, K. Syassen, U. Schwarz, M. Hanfland, G. Kh. Rozenberg, P. Gorodetsky, and M. P. Pasternak, Phys. Rev. Lett. **87**, 125501 (2001).
[14] J. A. Alonso, M. J. Martinez-Lope, M. T. Casais, M. A. G. Aranda, and M. T. Fernandez-Diaz, J. Am. Chem. Soc. **121**, 4754 (1999).
[15] J. A. Alonso, M. J. Martinez-Lope, M. T. Casais, J. L. Garcia-Munoz, and M. T. Fernandez-Diaz, Phys. Rev. B **61**, 1756 (2000).
[16] J. Pérez-Cacho, J. Blasco, J. Garcia, M. Castro, and J. Stankiewicz, J. Phys.: Condens. Matter **11**, 405 (1999).
[17] R. Lengsdorf, A. Barla, J. A. Alonso, M. J. Martinez-Lope, H. Micklitz, and M. M. Abd-Elmeguid, J. Phys.: Condens. Matter **16**, 3355 (2004).
[18] J.-S. Zhou, J. B. Goodenough, B. Dabrowski, P. W. Klamut, and Z. Bukowski, Phys. Rev. B **61**, 4401 (2000).
[19] T. Yamazaki, N. Takeshita, R. Kobayashi, H. Fukazawa, Y. Kohori, K. Kihou, C.-H. Lee, H. Kito, A. Iyo, and H. Eisaki, Phys. Rev. B **11**, 224511 (2010).
[20] J. L. García-Muñoz, M. Suaaidi, M. T. Martínez-Lope, and J. A. Alonso, Phys. Rev. B **52**, 13563 (1995).
[21] J. A. Alonso, M. J. Martinez-Lope, and M. A. Hidalgo, J. Solid State Chem. **116**, 146 (1995).
[22] I. V. Nikulin, M. A. Novojiov, A. R. Kaul, S. N. Mudretsova, and S. V. Kondrashov, Mater. Res. Bull. **39**, 775 (2004).
[23] M. T. Causa, R. D. Sanchez, M. Tovar, J. A. Alonso, and M. J. Martinez-Lope, Phys. Rev. B **68**, 024429 (2003).
[24] R. D. Sanchez, M. T. Causa, M. Tovar, J. A. Alonso, and M. J. Martinez-Lope, J. Magn. Magn. Mater. **272-276**, 390 (2004).
[25] X. Obradors, L. M. Paulius, M. B. Maple, J. B. Torrance, A. I. Nazzal, J. Fontcuberta, and X. Granados, Phys. Rev. B **47**, 12353 (1993).
[26] P. C. Canfield, J. D. Thompson, S.-W. Choeng, and L. W. Rupp, Phys. Rev. B **47**, 12357 (1993).
[27] L. F. Schneemeyer, J. K. Thomas, T. Siegrist, B. Batlogg, L. W. Rupp, R. L. Opila, R. J. Cava, and D. W. Murphy, Nature (London) **335**, 421 (1988).
[28] J. B. Goodenough, J. Solid State Electrochem. (to be published).
[29] J.-S. Zhou and J. B. Goodenough, Phys. Rev. Lett. **89**, 087201 (2002).
[30] J.-S. Zhou, J. B. Goodenough, and B. Dabrowski, Phys. Rev. Lett. **95**, 127204 (2005).
[31] D. Bloch, J. Phys. Chem. Solids **27**, 881 (1966).
[32] M. Amboage, M. Hanfland, J. A. Alonso, and M. J. Martinez-Lope, J. Phys.: Condens. Matter **17**, S783 (2005).
[33] J. L. García-Muñoz, M. Amboage, M. Hanfland, J. A. Alonso, M. J. Martinez-Lope, and R. Mortimer, Phys. Rev. B **69**, 094106 (2004).
[34] M. Medarde, J. Mesot, S. Rosenkranz, P. Lacorre, W. Marshall, S. Klotz, J. S. Loveday, G. Hamel, S. Hull, and P. Radaelli, Physica B **234-236**, 15 (1997).